



Fan Noise Source Diagnostic Test— Tone Modal Structure Results

Laurence J. Heidelberg
Glenn Research Center, Cleveland, Ohio

The NASA STI Program Office . . . in Profile

Since its founding, NASA has been dedicated to the advancement of aeronautics and space science. The NASA Scientific and Technical Information (STI) Program Office plays a key part in helping NASA maintain this important role.

The NASA STI Program Office is operated by Langley Research Center, the Lead Center for NASA's scientific and technical information. The NASA STI Program Office provides access to the NASA STI Database, the largest collection of aeronautical and space science STI in the world. The Program Office is also NASA's institutional mechanism for disseminating the results of its research and development activities. These results are published by NASA in the NASA STI Report Series, which includes the following report types:

- **TECHNICAL PUBLICATION.** Reports of completed research or a major significant phase of research that present the results of NASA programs and include extensive data or theoretical analysis. Includes compilations of significant scientific and technical data and information deemed to be of continuing reference value. NASA's counterpart of peer-reviewed formal professional papers but has less stringent limitations on manuscript length and extent of graphic presentations.
- **TECHNICAL MEMORANDUM.** Scientific and technical findings that are preliminary or of specialized interest, e.g., quick release reports, working papers, and bibliographies that contain minimal annotation. Does not contain extensive analysis.
- **CONTRACTOR REPORT.** Scientific and technical findings by NASA-sponsored contractors and grantees.

- **CONFERENCE PUBLICATION.** Collected papers from scientific and technical conferences, symposia, seminars, or other meetings sponsored or cosponsored by NASA.
- **SPECIAL PUBLICATION.** Scientific, technical, or historical information from NASA programs, projects, and missions, often concerned with subjects having substantial public interest.
- **TECHNICAL TRANSLATION.** English-language translations of foreign scientific and technical material pertinent to NASA's mission.

Specialized services that complement the STI Program Office's diverse offerings include creating custom thesauri, building customized data bases, organizing and publishing research results . . . even providing videos.

For more information about the NASA STI Program Office, see the following:

- Access the NASA STI Program Home Page at <http://www.sti.nasa.gov>
- E-mail your question via the Internet to help@sti.nasa.gov
- Fax your question to the NASA Access Help Desk at 301-621-0134
- Telephone the NASA Access Help Desk at 301-621-0390
- Write to:
NASA Access Help Desk
NASA Center for Aerospace Information
7121 Standard Drive
Hanover, MD 21076



Fan Noise Source Diagnostic Test— Tone Modal Structure Results

Laurence J. Heidelberg
Glenn Research Center, Cleveland, Ohio

Prepared for the
Eighth Aeroacoustics Conference
cosponsored by the American Institute of Aeronautics and Astronautics
and the Confederation of European Aerospace Societies
Breckenridge, Colorado, June 17–19, 2002

National Aeronautics and
Space Administration

Glenn Research Center

Acknowledgments

Acknowledgment is given to Daniel Sutliff, SEST, Inc., who wrote the data reduction, and acquisition programs, used in this investigation, under contract NAS3-00170. Acknowledgment is given to General Electric Aircraft Engines for designing the R4 model fan and providing it to NASA as the current technology bypass fan for this test. Also, GEAE designed and fabricated the three model OGV (stator) configuration and model nacelle used in this test under NASA Contract NAS3-26617, Task Order 7.

This report is a preprint of a paper intended for presentation at a conference. Because of changes that may be made before formal publication, this preprint is made available with the understanding that it will not be cited or reproduced without the permission of the author.

Available from

NASA Center for Aerospace Information
7121 Standard Drive
Hanover, MD 21076

National Technical Information Service
5285 Port Royal Road
Springfield, VA 22100

Available electronically at <http://gltrs.grc.nasa.gov/GLTRS>

Fan Noise Source Diagnostic Test—Tone Modal Structure Results

Laurence J. Heidelberg*
National Aeronautics and Space Administration
Glenn Research Center
Cleveland, Ohio 44135

ABSTRACT

This investigation is part of a test series that was extremely comprehensive and included aerodynamic and acoustic testing of a fan stage using two different fan rotors and three different stator designs. The test series is known as the Source Diagnostic Test (SDT) and was conducted by NASA Glenn as part of the Advanced Subsonic Technology (AST) Noise Reduction Program. Tone mode measurements of one of the rotors with three different stators were made. The stator designs involve changes in vane count and sweep at constant solidity. The results of both inlet and exhaust tone mode measurements are presented in terms of mode power for both circumferential and radial mode orders. The results show benefits of vane sweep to be large, up to 13 dB in total tone power. At many conditions, the increase in power due to cutting on the rotor/stator interaction is more than offset by vane sweep. The rotor locked mode is shown as an important contributor to tone power when the blade tip speed is near and above Mach one. This is most evident in the inlet when the direct rotor field starts to cuton.

INTRODUCTION

A series of tests known as the Source Diagnostic Test (SDT) was conducted by NASA Glenn as part of the Advanced Subsonic Technology (AST) Noise Reduction Program. The AST program is a partnership with NASA, the FAA, and the U.S. aerospace industry for the purpose of reducing aircraft noise. This paper will present the results of both inlet and exhaust tone mode measurements of one of the rotors with three different stators. The stators were designed to investigate the effects of vane count (cutoff of rotor/stator interaction at Blade Passing Frequency, BPF), and vane sweep angle on both tone and broadband noise. These measurements were made using a continuously rotating acoustic rake technique (refs. 1 and 2). Both circumferential, m and radial mode, n orders are measured and presented in terms of sound power. These measurements can reveal much about fan source noise, its propagation in the engine ducts, explain far-field directivity patterns, and help verify fan source noise prediction codes.

APPARATUS AND PROCEDURE

Fan Models

The SDT fan stage used one of two different rotors and three different stators, but only the rotor designated R4 was used

during mode measurement. Table I shows the design parameters for the R4 rotor, as well as the three stators sets. The SDT fan stage was tested with two radial stators, 54-vane cutoff at BPF and 26-vane cuton. The motivation for the lower vane count stator was to reduce fan broadband noise (ref. 3). In addition, a 26-vane swept stator (30° sweep) was tested. Stator sweep has been shown to reduce both fan tone and broadband noise levels (refs. 4–6). These three stators were designed for equivalent aerodynamic performance and had essentially the same solidity.

Mode Measurement

A continuously rotating microphone technique described in refs. 1 and 2 was used. The mode measurement system installed on the inlet is shown in figure 1. The same system installed in the fan exhaust is shown in figure 2. The rotating rake uses a control system slaved to the fan shaft to rotate at exactly 1/200th of the fan speed as if it were geared to the fan shaft. In the rotating frame of reference, each spinning circumferential mode order is Doppler shifted inversely proportional to its spin rate. Thus, each circumferential order is separated by 0.005 shaft orders in frequency. The radial order is determined by a least squares curve fit using the basis functions from the hard wall boundary condition of the Bessel's equation of all cuton radial orders plus the first cutoff order to the measured complex radial profile. In order to resolve the highest radial order that can propagate in the inlet, at 2BPF, 14 radial measurements were used, while only 8 were needed in the exhaust. These microphone signals are brought across the rotating frame by FM telemetry.

Several improvements in this mode measurement technique have been made since its first implementation reported in refs. 7–9. These improvements were developed during tests on a large low speed fan rig (Active Noise Control Fan – ANCF). These improvements involve the installation of aluminum foam windscreens over the microphones to lower self-noise, thus improving signal to noise ratio and additional foam shields on the exhaust rake to attenuate the effects of the rotor wakes and their interactions with the vanes on the microphones. The locations of the mode measurement planes are also shown in figure 3. The inlet measurements were taken at the throat (minimum diameter). The exhaust measurements were taken in a plane just inside the nozzle exit.

Test Conditions

The fan models were run in the NASA Glenn 9' x 15' Low Speed Wind Tunnel at a Mach number of 0.10. The fan was operated at six different speeds for the mode measurements, as shown in Table 2 that include nominal approach, cutback, and takeoff conditions. A slightly larger nozzle exit area was used

*Senior Research Engineer, Senior Member AIAA

for exhaust measurements to compensate for rake blockage. All tests were run with ducts in a hard wall (no acoustic treatment) configuration.

RESULTS AND DISCUSSION

The complete modal structure (circumferential and radial orders) for BPF and 2BPF were measured. Both inlet and exhaust duct modes are presented in terms of sound power, PWL, referenced to 10^{-12} watts. An example of the 2BPF modal structure for the exhaust is shown in figure 4 in the form of a 3-D bar graph. This figure is for cutback power setting. The mode orders are displayed on the horizontal axes, and the power on the vertical axis. The back row represents the sum of the radial orders in each circumferential order. This m-order power distribution plot will be used to describe the modal structure for most of this report due to its simplicity. The rotor/stator interaction m orders are easily seen in the back row standing well above the extraneous modes (other than rotor/stator interaction modes).

Exhaust Mode Power

The exhaust m order power plot at BPF for all three stators at approach power (61.7% design fan speed) is shown in figure 5. The rotor/stator interaction orders are highlighted in red in this and all following plots of this type. Both 26 vane stators show large interaction power at $m = -4$, with the radial vanes showing the highest levels. The benefit of sweep for the interaction mode, at this condition is about 5dB. The 54-vane stator has no interaction mode and thus has very low total tone power. The extraneous modes for all configurations are low and contribute little to total tone power when an interaction mode is present. The same plot for the cutback power (87.5% speed) setting is shown in figure 6. Similar results to the previous figure are shown here except that the benefit due to sweep is much larger, almost 15 dB, and low levels of $m = 22$ are just cutting on. Finally, the takeoff power (100% speed) setting is shown in figure 7. Here the total tone power for both radial vane stators is nearly the same. For the 26-vane stator case the total power is mostly due to the $m = -4$ mode while in the 54-vane case, it is $m = 22$ (rotor locked) that controls. The benefit of sweep shows up in both interaction modes with reductions of 8 dB for $m = -4$ and 15 dB for $m = 22$. It is interesting to compare the two radial vane stators with respect to the $m = 22$ mode. The higher count, 54, has a power level more than 3 dB higher. This may be an indication that higher vane counts produce higher interaction mode power.

The 2BPF results in the exhaust, for all three power settings, are shown in figures 8–10. At approach power both 26 vane stators have two interaction modes, $m = -8$ and 18. The benefit of sweep can be seen in the almost 10 dB in total tone power reduction. The 54 vane radial stator has only one interaction mode at $m = -10$. At cutback, the 26-vane stators now have three interaction modes, $m = -34, -8, 18$. The reductions of these modes, for the swept vanes are so large, as to make it difficult to distinguish them from the extraneous modes. The 54-vane stator has only one interaction mode, $m = -10$. The total tone power for this stator falls between the

other two configurations. The takeoff power results (fig. 12) are similar to cutback except at this speed the $m = 44$ is cuton. Although this rotor locked mode is cuton, it is below the noise floor for the swept vanes and highest for the 54-vane case, similar to the $m = 22$ BPF results.

Inlet Mode Power

The inlet m-order power distribution at BPF, for all three stator configurations at approach power is shown in figure 11. Here, as with the exhaust only the 26-vane stators have a cuton interaction mode, $m = -4$. The swept vanes show a reduction of 9 dB in mode power. A comparison to the exhaust results (fig. 7) indicates the inlet has significantly lower mode and tone power levels. This trend grows with speed, and will be discussed further, in a latter section of this report. Figure 12 shows the BPF modal power distribution for the cutback condition. The interaction mode has been reduced almost 13 dB due to sweep, to the point where it is at the level of the extraneous modes. Unfortunately, inlet data for the takeoff power setting was not obtained.

The 2BPF modal power distributions are shown in figures 13 and 14. There are two propagating interaction modes at approach for the 26-vane stators, $m = -8$ and 18, and one for the 54-vane stator, $m = -10$. The swept vanes again demonstrated a large power reduction compared to the radial vanes, with the $m = -8$ mode below the noise floor. The 54-vane stator has a very low power level for the interaction mode, just above the extraneous modes. At cutback power (fig. 14) the 26-vane stators have higher levels of the same two modes ($m = -8$ and 18). The benefit of sweep is almost 5 dB in total power. Although a new mode is cuton at this speed, $m = -34$, it is not evident in the data. This is probably due to the difficulty of counter-rotating modes to propagate through the swirl zone and the rotor blades (ref. 10). It is likely, that for the same reason, the interaction mode level for the 54-vane configuration is at the levels of the extraneous modes.

Interaction Mode Power Variation with Fan Speed

The exhaust interaction mode power levels at BPF are plotted for all three stators as a function of fan speed in figure 15. The individual and the sum of the modes are plotted. For both 26-vane stators the $m = -4$ mode controls the power. The swept vanes show a benefit at all speeds with the benefit increasing with speed such that there is little change in power over the full speed range. Although the 54-vane stator is a cutoff design, at cutback speed the $m = 22$ cuts on for all stators (the rotor wake trace speed on the stators is sonic). This mode carries as much power as the $m = -4$ of the 26 radial vane stator at takeoff speed. Perhaps the higher vane count is responsible for the higher level of this rotor locked mode. The 2BPF modal power variation with speed is shown in figure 16. The large number of interaction modes at these frequencies is obvious especially for the 26 vane cases. For both 26-vane cases there is an increase in modal power with speed up to cutback for all modes. Above cutback most modes decrease with speed, as does the sum of the interaction modes. The 54-vane stator shows a marked drop in power at just above cutback. This speed happens to be where the $m = 44$ (rotor locked) mode cuts on. The trend of the other

interaction modes to decrease as the rotor locked mode cuts on (sonic tangential fan tip speed) is evident in the other stators and also at BPF.

The inlet interaction modes and $m = 22$ (direct rotor field) at BPF are shown as a function of fan speed in figure 17. The 26-vane stators have only one interaction mode, $m = -4$. The power levels for the swept vanes are generally about 10 dB lower than the radial vanes. These levels peak between approach and cutback speed. The $m = -4$ mode has relatively low levels in the inlet in part due to propagation effects through the swirl zone between the rotor and stator, and through the rotor itself. Counter-rotating modes (negative) are attenuated more than the co-rotating modes in the inlet and thus are generally chosen as the interaction mode orders by selecting an appropriate vane count. The $m = 22$ mode shown is not an interaction mode as in the exhaust, but rather the direct rotor potential field which can propagate without loss when it rotates at above sonic speed. Actually, for the highest speed shown this mode (22,0) is not cuton but approximately 3% below cuton speed. This is possible since this mode has a low decay rate and is very strong at the fan. In addition, the duct diameter is smaller at the throat than the fan face thus the average cutoff ratio between the throat and the fan is still closer to unity.

The rotating rake technique used here generally cannot measure the rotor locked mode in the inlet due to interference of the rake wake interaction with the rotor. In this case, the $m = 22$ mode is much stronger than the interference and thus, the interference is not likely to cause a significant error. The relative strength of the interference and the rotor locked modes is shown in figure 18. Here the pressure levels, extrapolated to the wall of the mode (22,0) are plotted as a function of corrected fan speed for all three stator configurations. The speed just above cutback was almost 10 dB above the previous point, indicating that the rotor locked mode is much stronger than the interference. Further verification of the $m = 22$ measurements was provided by the comparison to wall pressure measurements from reference 11 with good agreement. All three stators show almost exactly the same level of power in figure 17. This makes sense if the source of $m = 22$ is the rotor and not a rotor/stator interaction that would be expected to change with stator design. This very strong rotor locked mode controls the tone total power for all stator configurations above cutback power. The 54-vane stator has no propagating interaction modes at BPF.

The inlet 2BPF modal power variation with speed is shown in figure 19. There are two interaction modes, $m = -8$ and 18 for the 26 vanes stators with $m = 18$ being dominate. These same two modes in the exhaust had nearly equal power while in the inlet $m = -8$ is 15 to 20 dB lower than $m = 18$ for the 26-vane radial stator. This is another example of rotor/swirl zone

propagation effects for negative m orders. The 54-vane stator has only one interaction mode, $m = -10$ with levels that are very low, consistent with negative mode orders. All three stators have nearly the same level (120+ dB) of the rotor locked mode, $m = 44$ as was the case for $m = 22$ at BPF. Although the BPF rotor locked mode was slightly below cuton, in this case $m = 44$ is just barely cuton. The rotor locked mode at 2BPF is lower than the BPF but still has a significant effect on tone noise above cutback.

A comparison of the inlet to exhaust mode power level at BPF (fig. 17 vs. 15) reveals the exhaust levels are generally much higher. A notable exception to this is when the rotor locked mode starts to appear in the inlet. Similar trends to the BPF comparisons can be seen for 2BPF by comparing figure 19 to figure 16. The inlet rotor locked mode for 2BPF, $m = 44$, is less important here.

CONCLUDING REMARKS

The effect of cutting on rotor/stator interaction fan noise at BPF (going from 54 to 26 count) for radial vanes is to significantly increase tone noise for both inlet and exhaust at most power settings and for BPF orders one and two. A notable exception was at power settings above cutback, there was no significant difference in tone power due to the cuton of a strong rotor locked mode. The effect of sweeping the stators (comparing the 26-vane radial to 26-vane swept) was dramatic with 3–13 dB reduction in total tone power. Even more dramatic reductions for the swept vanes can be seen in terms of individual interaction m -orders with power reductions with differences over 20 dB. In some cases, generally at higher power setting, the 26-vane cuton swept stator had lower tone power levels than the 54-vane cutoff stator. An additional benefit of swept stators was a reduction of broadband noise. The tradeoff between tone and broadband noise can be seen in detail in reference 11, where the EPNL levels for all three stators are compared. The ranking order (highest to lowest), in terms decreasing noise was: 26-vane radial, 54-vane radial, and 26-vane swept. From an overall point of view, the 26-vane radial stators increased tone noise more than it decreased broadband, while the 26-vane swept stator substantially decreased broadband noise with little change in tone noise.

An interesting and important feature of these data are the high levels of rotor locked modes in both the inlet and exhaust at speeds above cutback. This is most notable was in the inlet at BPF where the $m = 22$ mode is responsible for total tone power increases of up to 20 dB. Since, at the inlet measuring station $m = 22$ is theoretically cutoff (a decaying field), the source levels of this mode were still larger at the fan face. This rotor locked mode might be a good candidate for active noise control since it has only one radial order.

REFERENCES

1. Heidelberg, L.J. and Hall, D.G., "Acoustic Mode Measurement in the Inlet of a Model Turbofan Using a Continuously Rotating Rake," *Journal of Aircraft*, Vol.32, No. 4, 1995, pp.761-767.
2. Hall, D., et al., "Acoustic Mode Measurement in the Inlet of a Model Turbofan Using a Continuously Rotating Rake: Data Collection/Analysis Techniques," AIAA-93-0599 (NASA TM-105936). January, 1993.
3. Ganz, U., Joppa, P. Patten, T., and Scharpf, D., "Boeing 18-inch Fan Broadband Noise Test," NASA/CR-1998-208704, 1998.
4. Kazin, S.B., "Radially Leaned Outlet Guide Vanes for Fan Source Noise Reduction," NASA CR-134486, November 1973.
5. Envia, E., Huff, D.L., and Morrison, C.R., "Analytical Assessment of Stator Sweep and Lean in Reducing Rotor-Stator Tone Noise," AIAA-96-1791, May 1996.
6. Woodward, R.P., Elliott, D.M., Hughes, C.E., and Berton, J.J., "Benefits of Swept and Leaned Stators for Fan Noise Reduction," AIAA-99-0479, 1998.
7. Heidelberg, L.J., et al., "A Unique Ducted Fan Test Bed for Active Noise Control and Aeroacoustics Research," AIAA Paper 96-1740, May 1996; also NASA TM-107213.
8. Sutliff, D.L., Nallasamy, M., Heidelberg, L.H., Elliott, D.M., "Baseline Acoustic Levels of the NASA Active Noise Control Fan Rig," AIAA Paper 96-1745, May 1996; also NASA TM-107214.
9. Heidelberg, L.J., and Elliot, D.M., "A Comparison of Measured Tone Modes for Two Low Noise Propulsion Fans," AIAA-2000-1989, June 2000; also NASA/TM-2000-210231.
10. Hanson, D.B., "Acoustic Reflection and Transmission of 2-Dimensional Rotors and Stators, Including Mode and Frequency Scattering Effects," NASA/CR-1999-208880, March 1999.
11. Premo, J.W., "Fan Noise Source Diagnostic Test—Circumferential Mode Measurement Results," AIAA-2001-2429, June 2002.
12. Woodward, R.P., et al., "Fan Noise Source Diagnostic Test—Far-field Acoustic Results," AIAA-2002-2427, June 2002.

Table 1 – Source Diagnostic Test Design Parameters

<u>Rotor</u>				
ROTOR	NO. BLADES	L. E. SWEEP	DESIGN TIP SPEED M/S (FT./S)	DESIGN STAGE PR
R4	22	0 ⁰	370 (1215)	1.47

<u>Stator</u>				
STATOR	NO. VANES	L. E. SWEEP	ASPECT RATIO	SOLIDITY
Radial Baseline	54	0 ⁰	3.51	1.52
Radial Low-Count	26	0 ⁰	1.67	1.51
Swept	26	30 ⁰	1.67	1.53

Table 2 – Fan Test Speeds

Corrected Speed, RPM	Percent Speed	Corrected Tangential Tip Speed, ft/sec	Condition
6329	50	608	
7809	61.7	750	Approach
9493	75	911	
11075	87.5	1063	Cut Back
11391	90	1093	
12657	100	1215	Take Off



Figure 1. A photograph of the rotating rake system installed on the fan inlet.



Figure 2. A photograph of the rotating rake system installed on the fan exhaust.

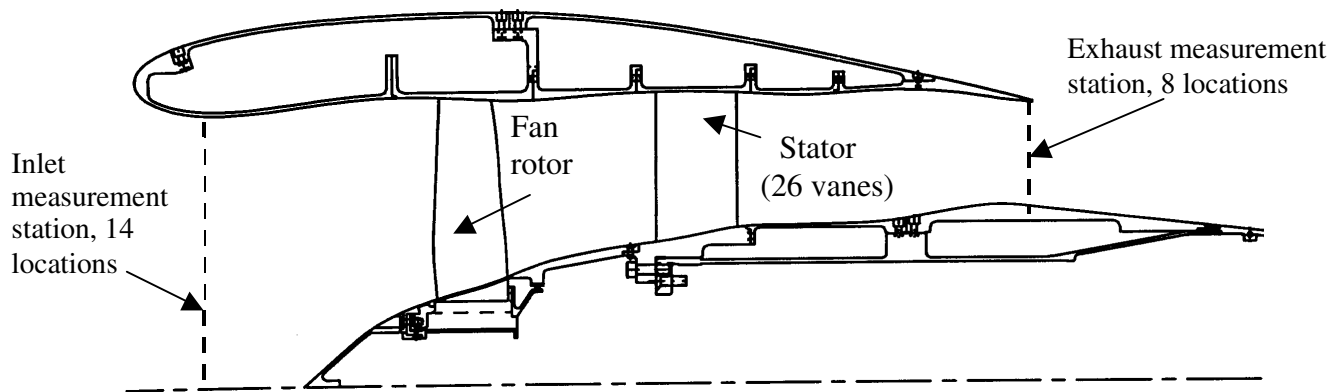


Figure 3. Location of mode measurement stations.

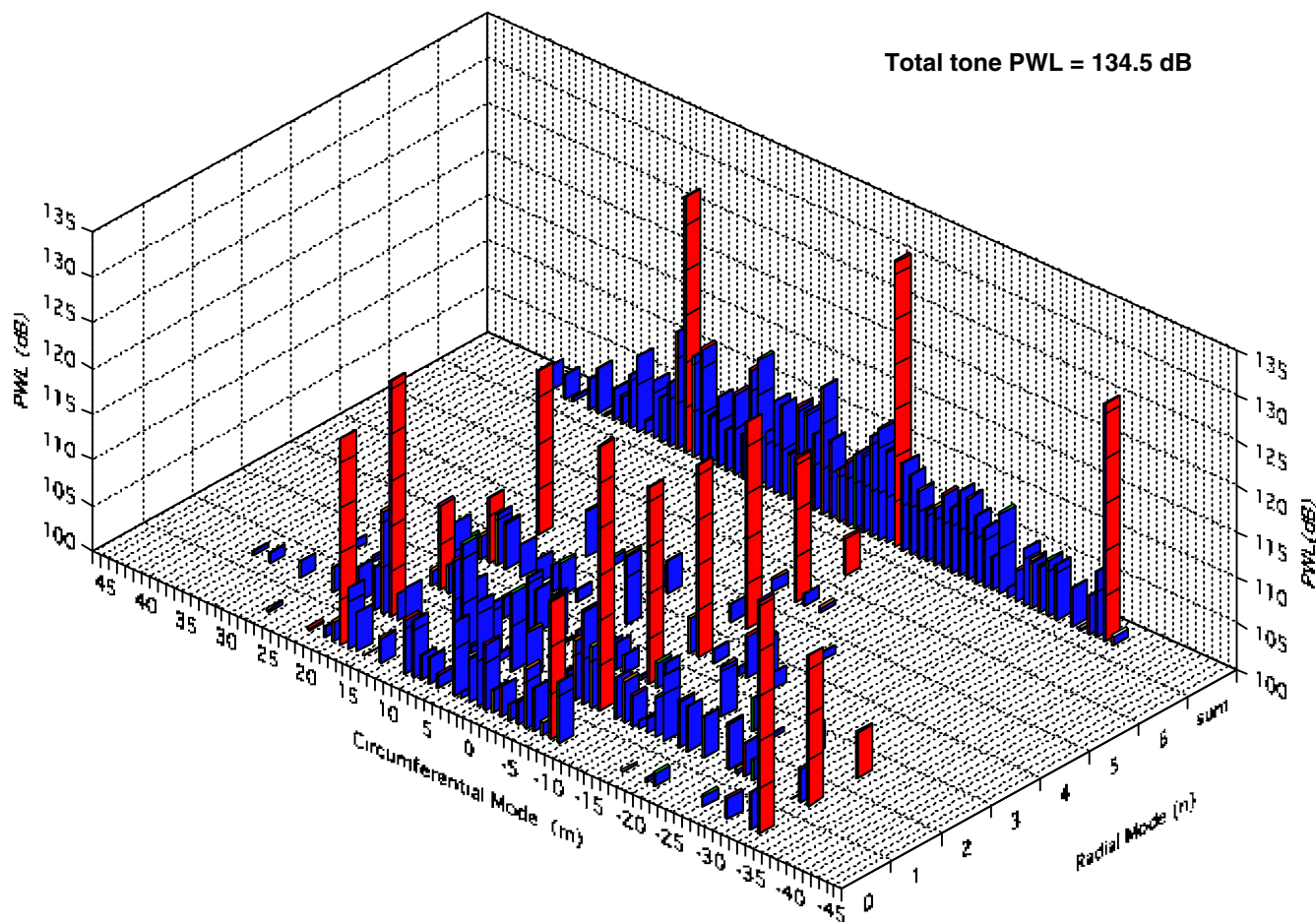
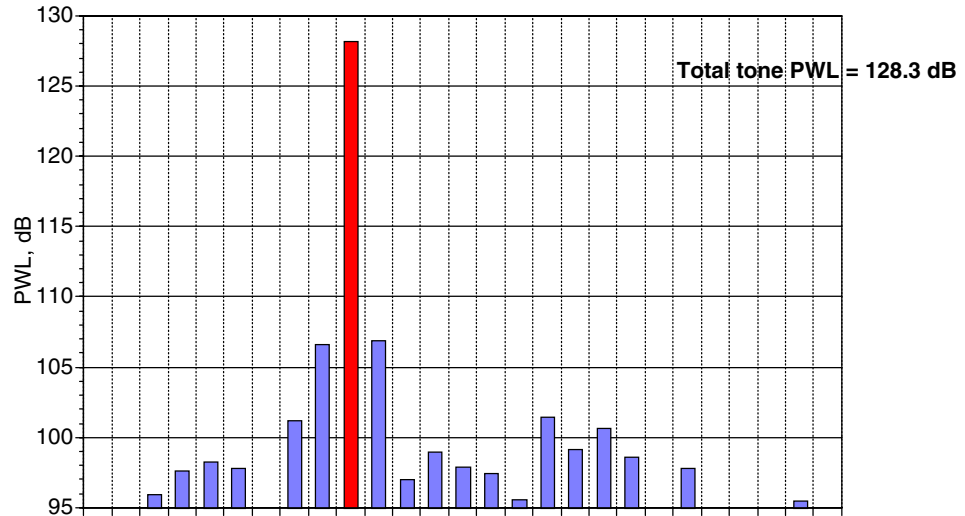
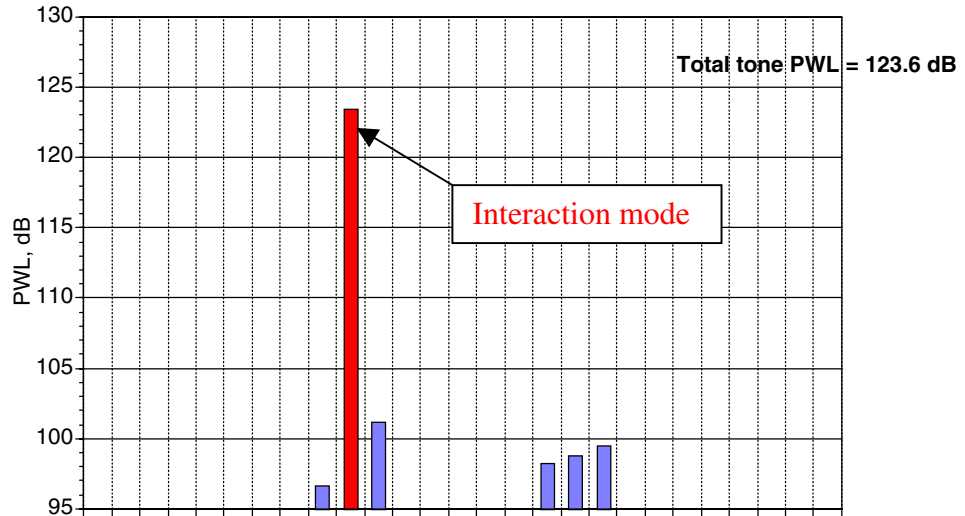


Figure 4. Typical complete modal structure, 2BPF in the exhaust for the 26 vane radial stator at cutback.

26 Radial Vanes



26 Swept Vanes



54 Radial Vanes

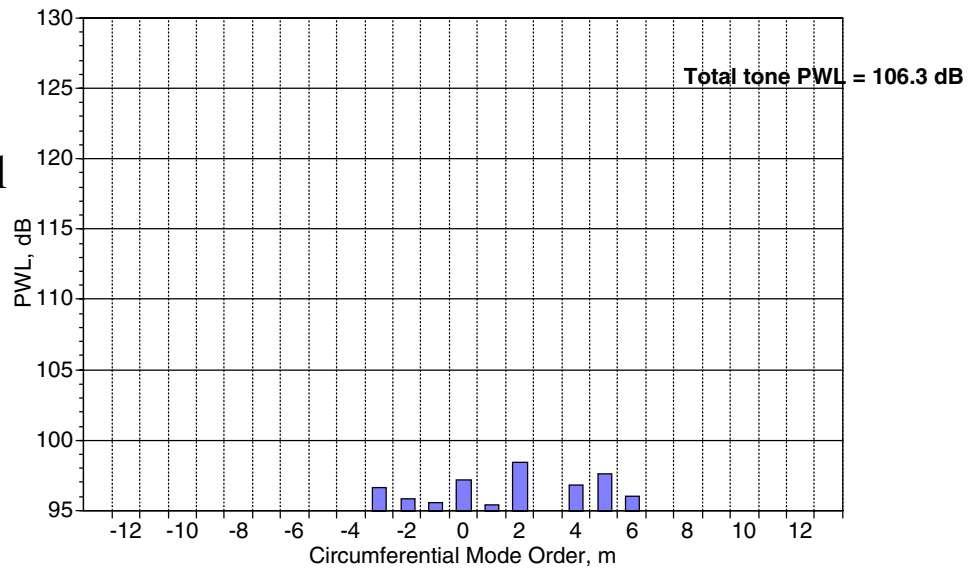
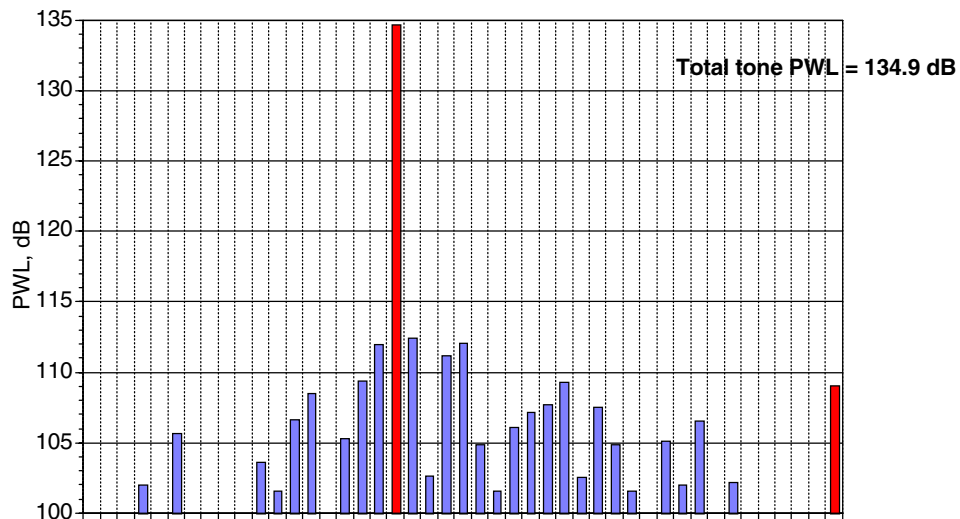
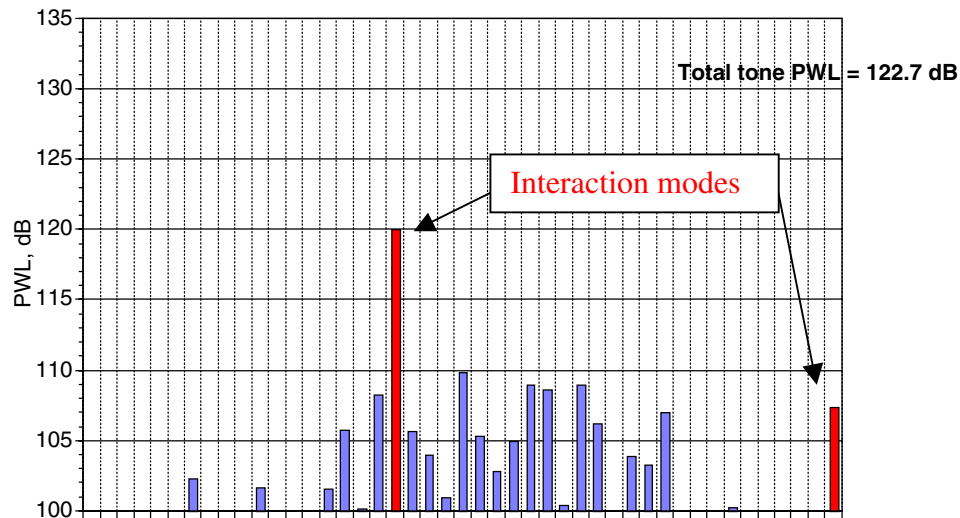


Figure 5. Exhaust BPF modal power distribution at approach, 61.7% speed.

26 Radial Vanes



26 Swept Vanes



54 Radial Vanes

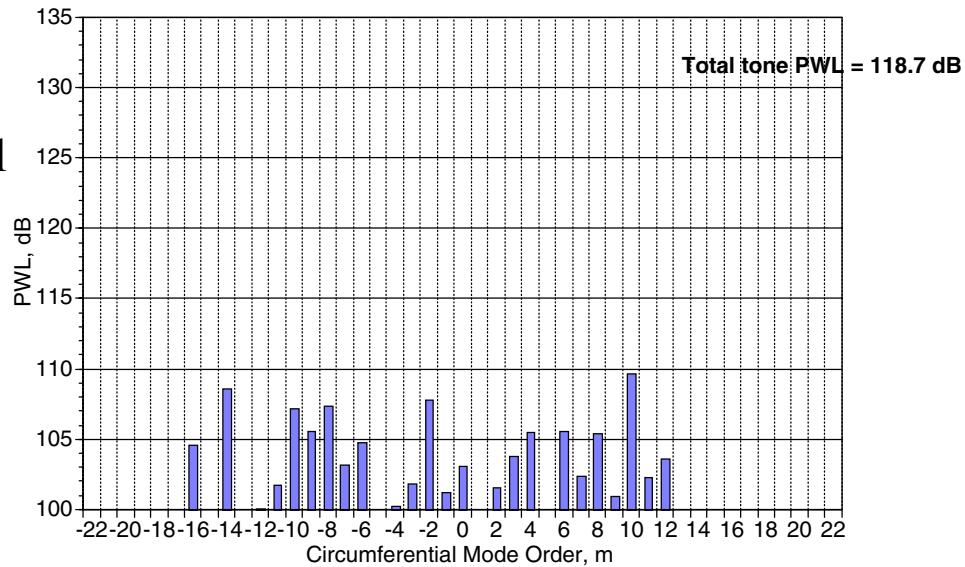


Figure 6. Exhaust BPF modal power distribution at cutback, 87.5% speed.

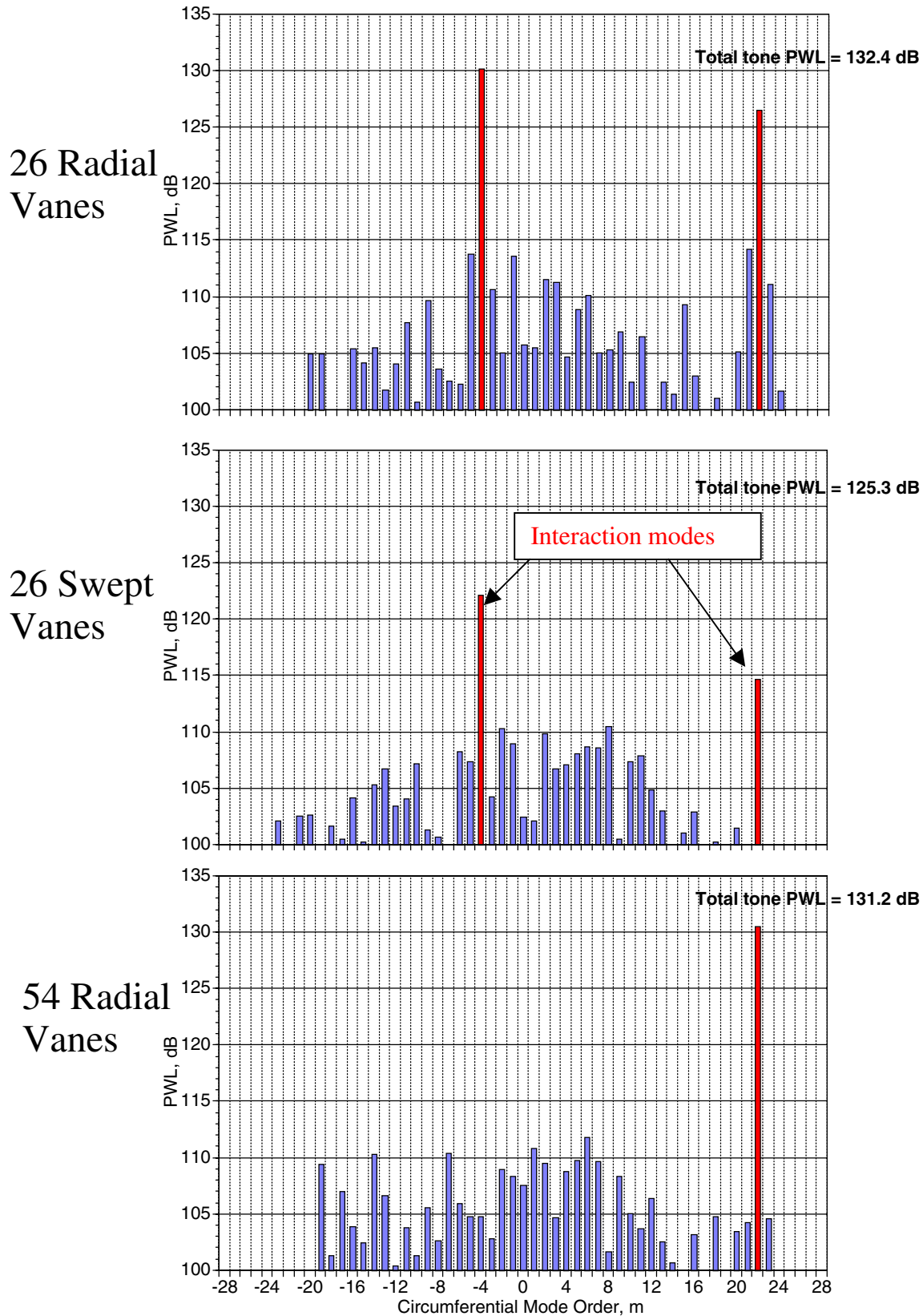
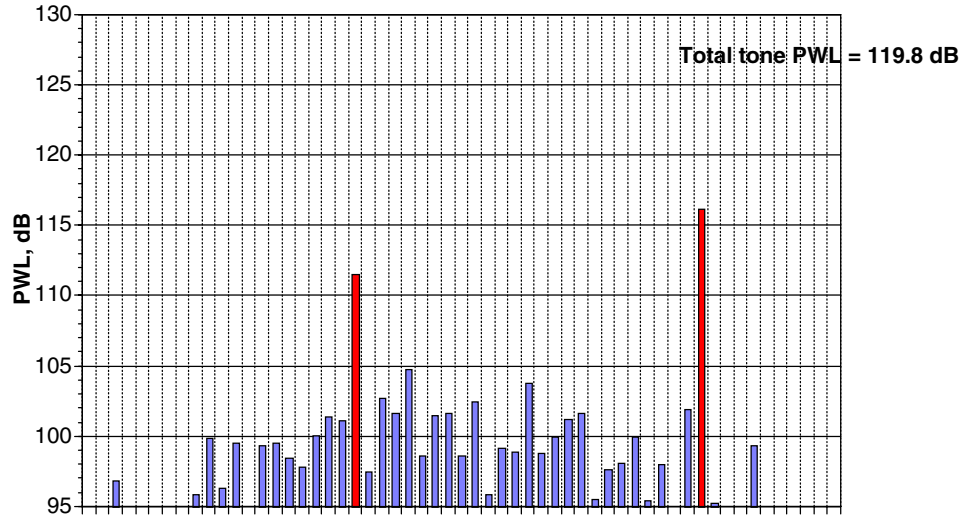
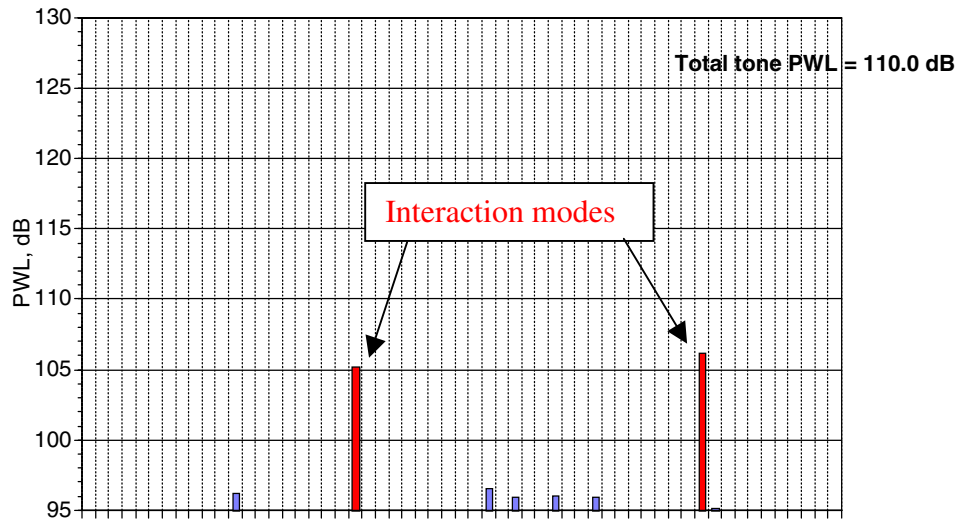


Figure 7. Exhaust BPF modal power distribution at takeoff, 100% speed.

26 Radial Vanes



26 Swept Vanes



54 Radial Vanes

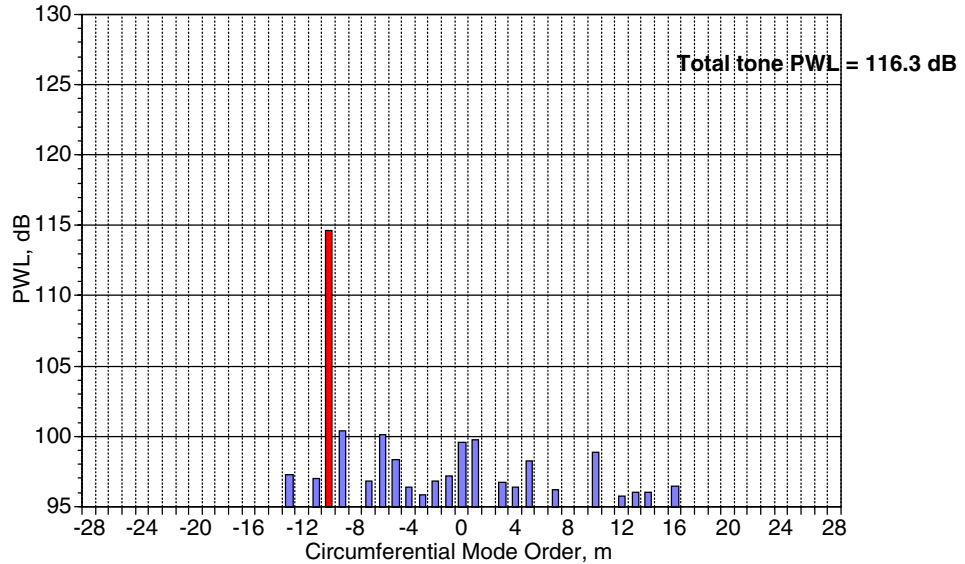


Figure 8. Exhaust 2BPF modal power distribution at approach, 61.7% speed.

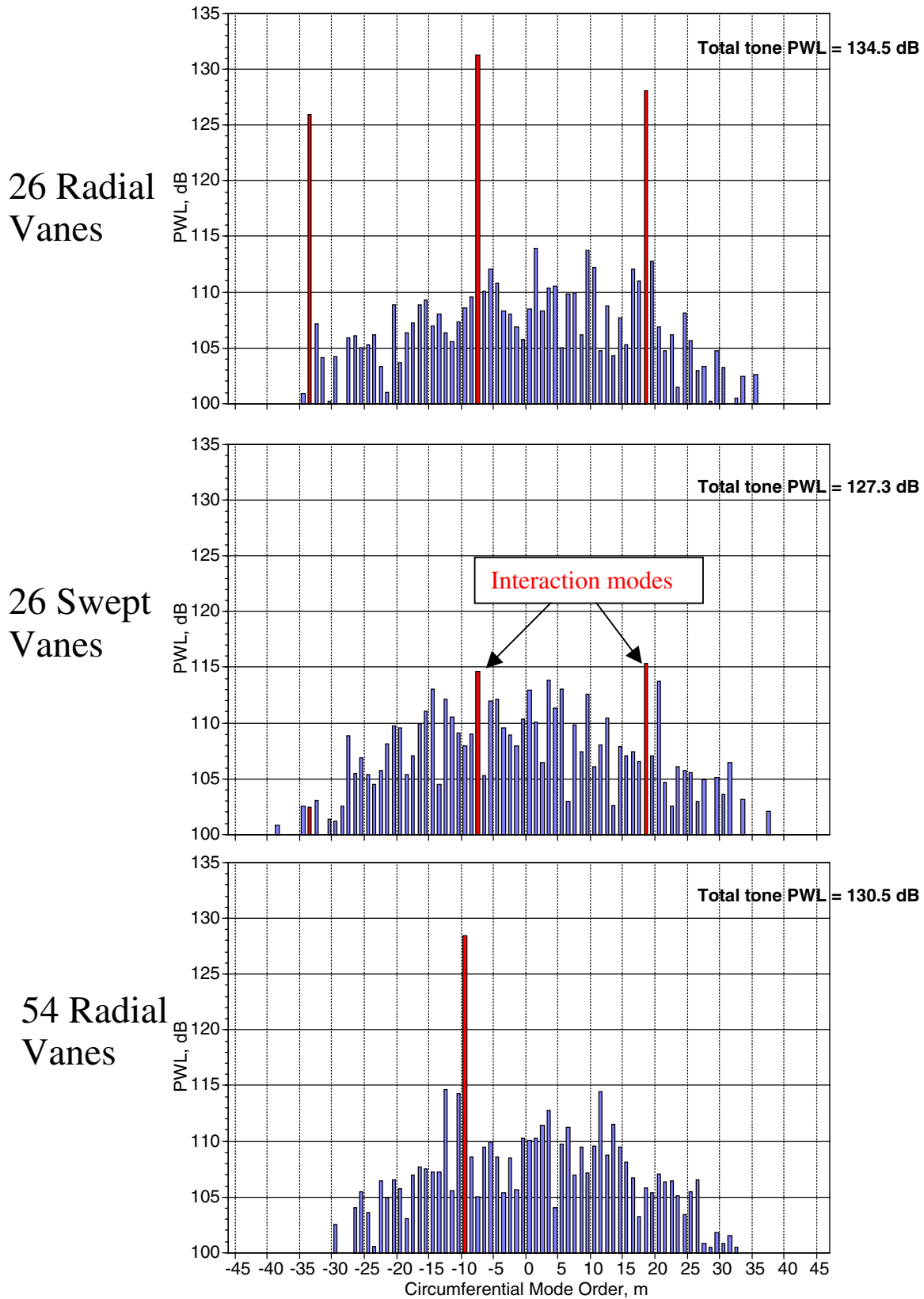
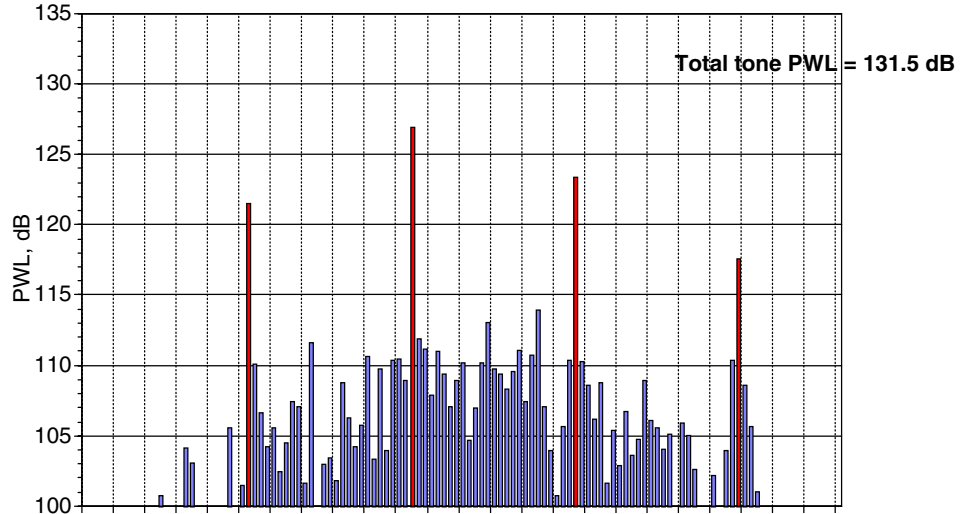
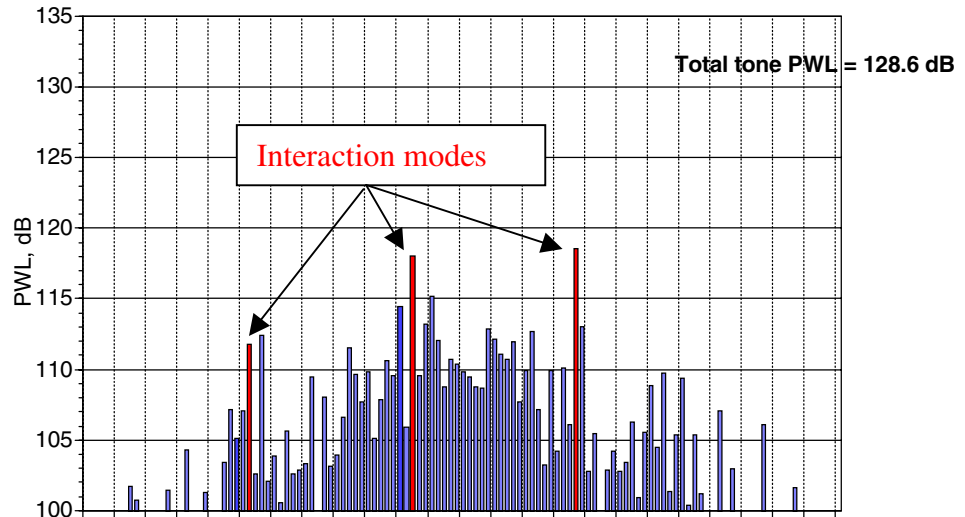


Figure 9. Exhaust 2BPF modal power distribution at cutback, 87.5% speed.

26 Radial Vanes



26 Swept Vanes



54 Radial Vanes

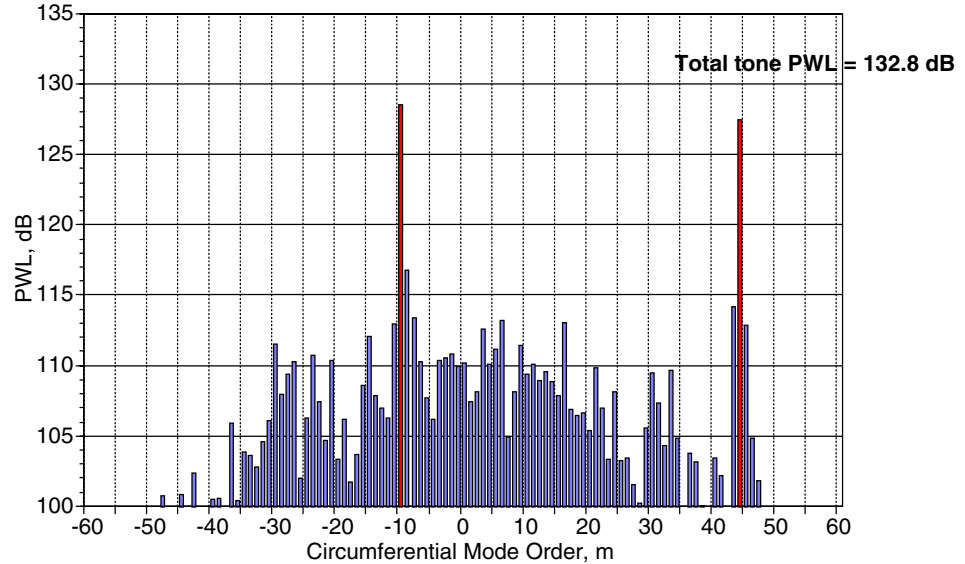
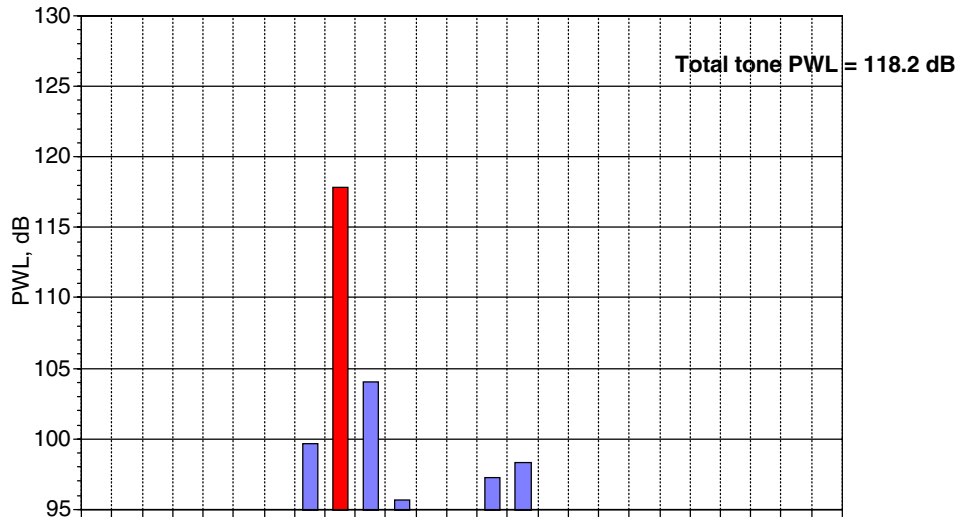
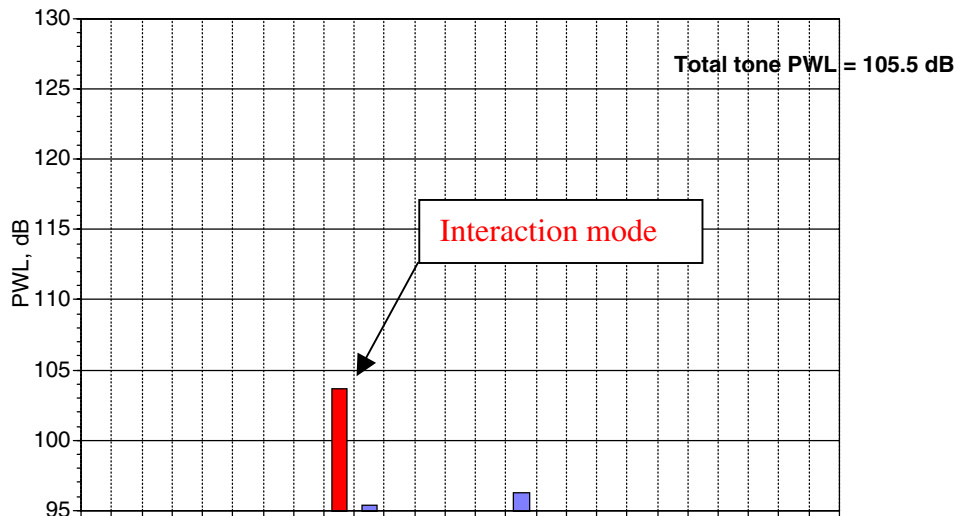


Figure 10. Exhaust 2BPF modal power distribution at takeoff, 100% speed.

26 Radial Vanes



26 Swept Vanes



54 Radial Vanes

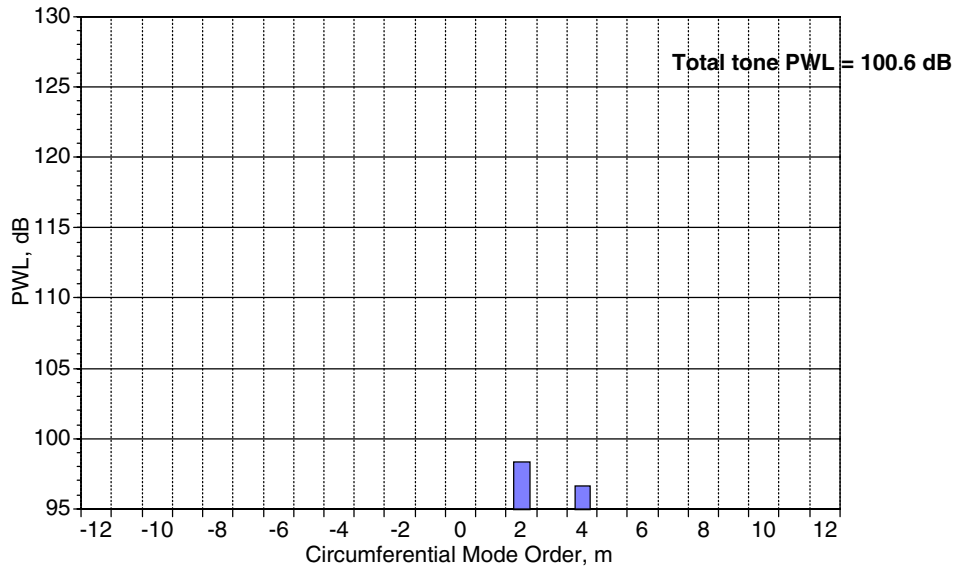
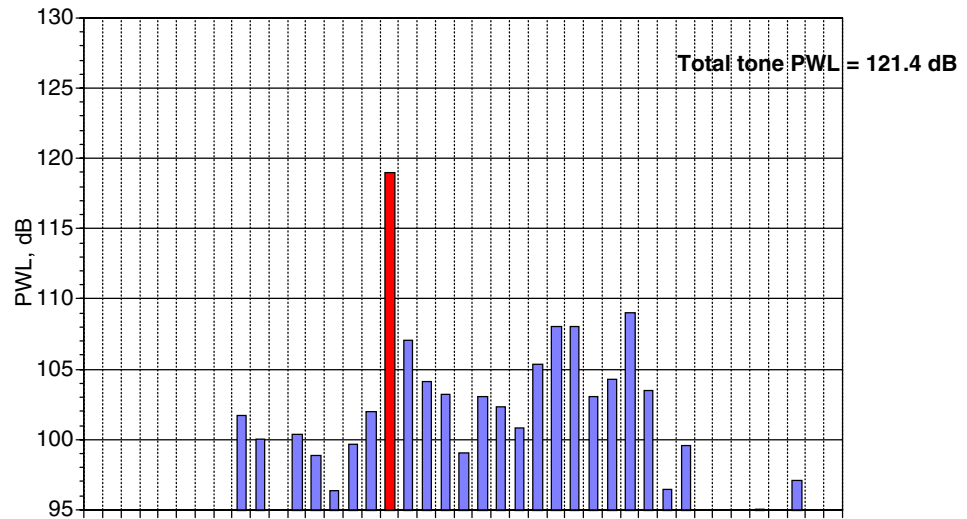
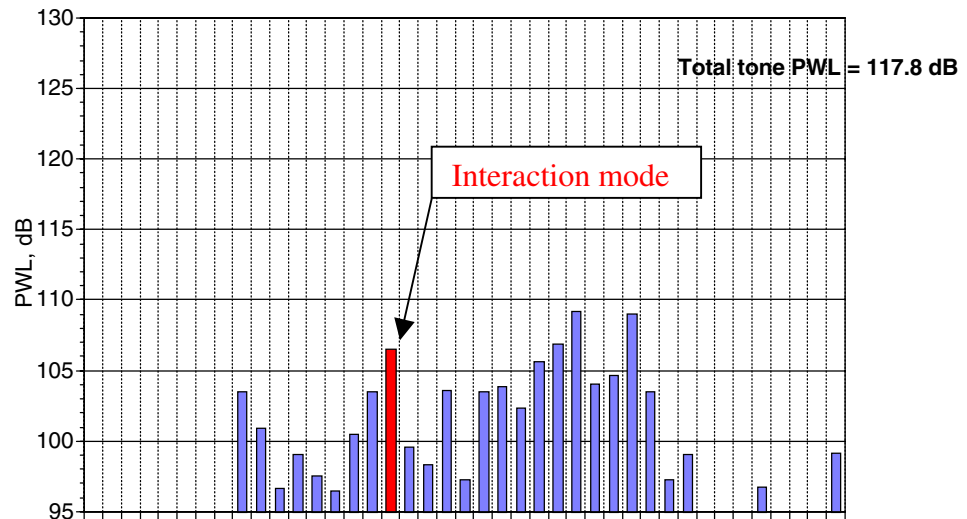


Figure 11. Inlet BPF modal power distribution at approach, 61.7% speed.

26 Radial Vanes



26 Swept Vanes



54 Radial Vanes

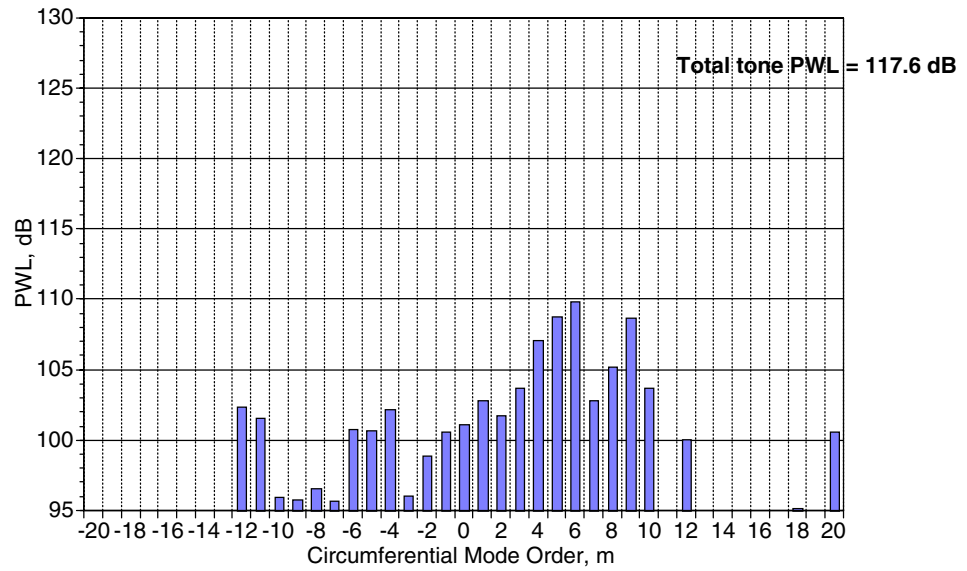
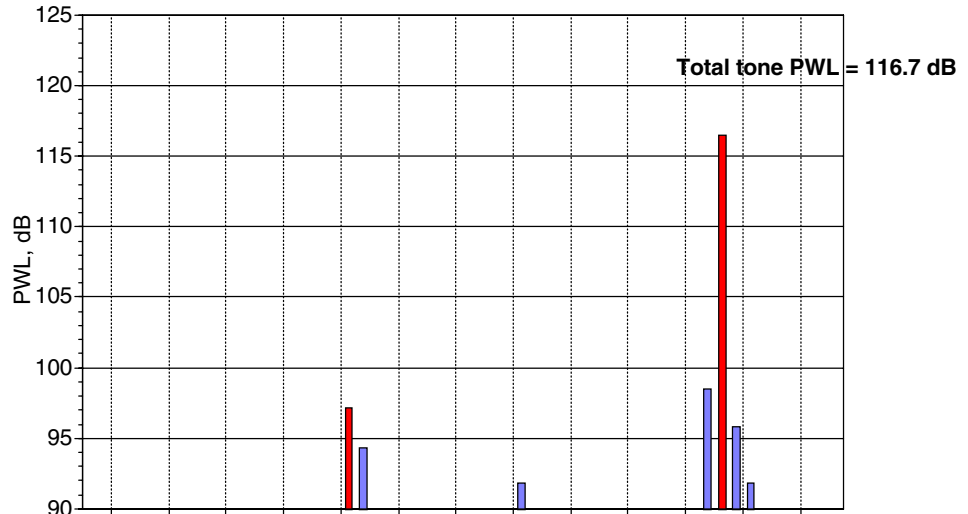
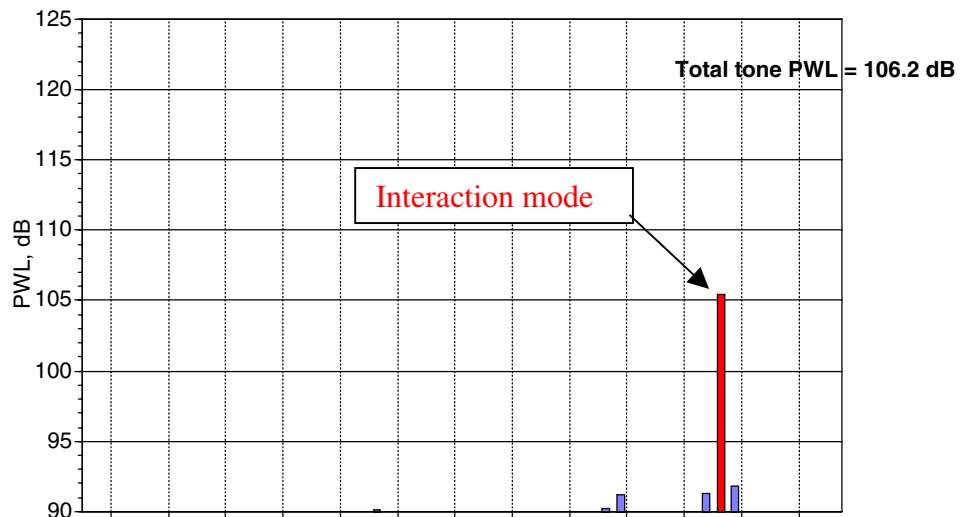


Figure 12. Inlet BPF modal power distribution at cutback, 87.5% speed.

26 Radial Vanes



26 Swept Vanes



54 Radial Vanes

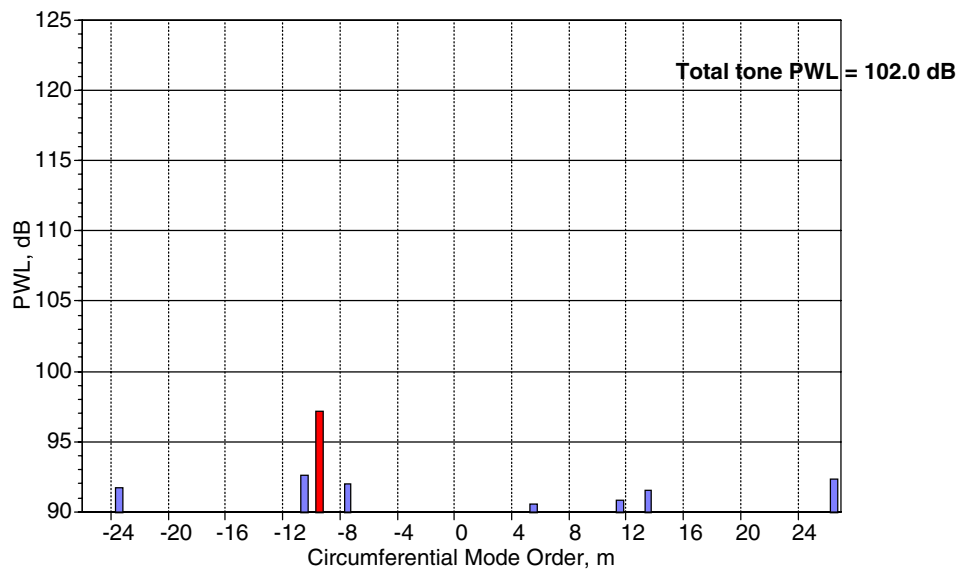
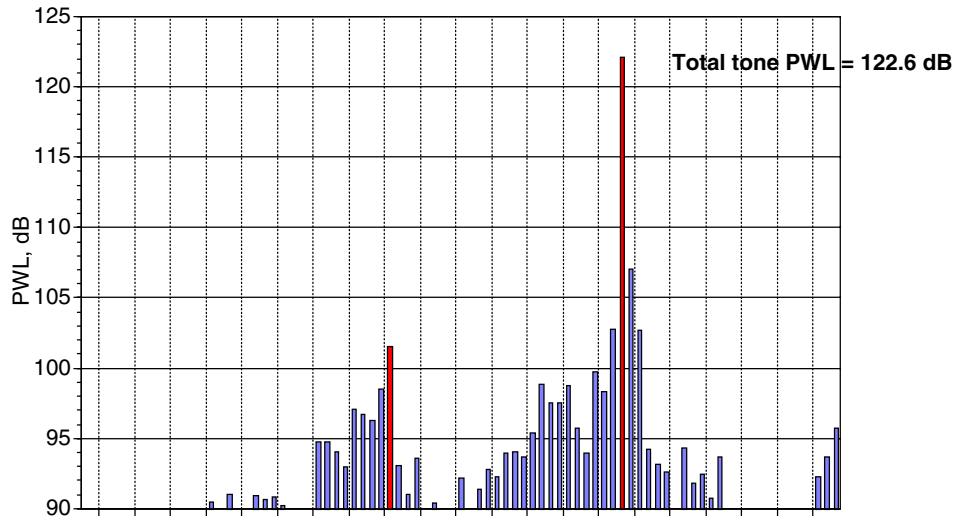
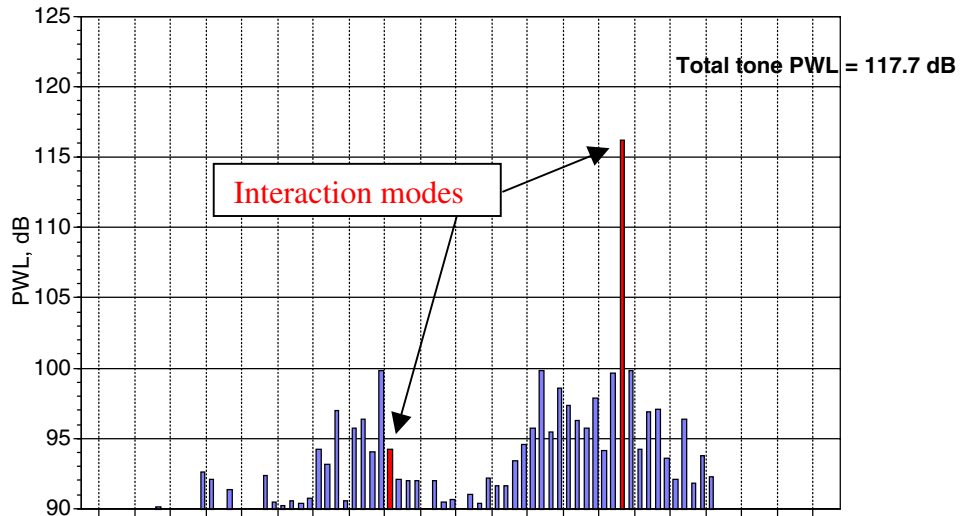


Figure 13. Inlet 2BPF modal power distribution at approach, 61.7% speed.

26 Radial Vanes



26 Swept Vanes



54 Radial Vanes

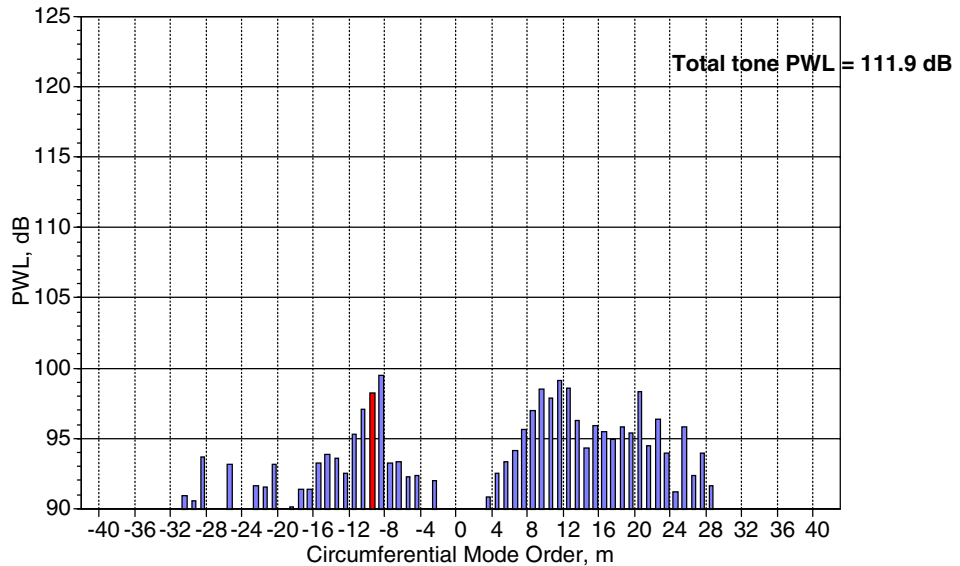
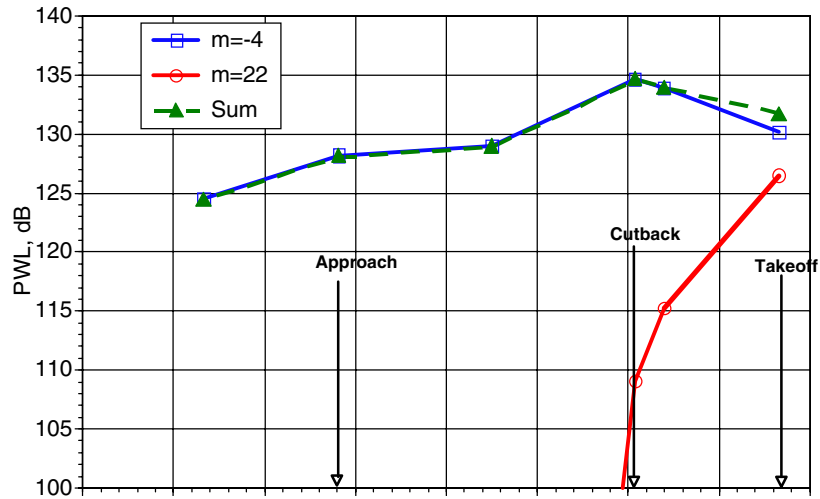
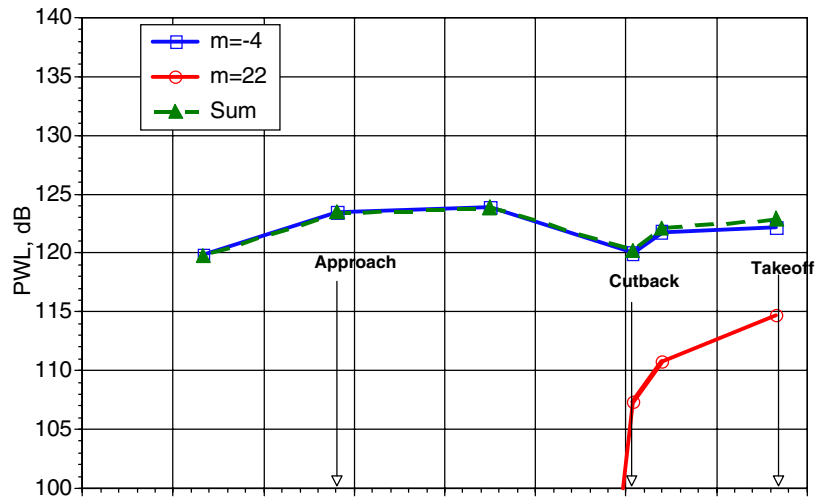


Figure 14. Inlet 2BPF modal power distribution at cutback, 87.5% speed.

26 Radial Vanes



26 Swept Vanes



54 Radial Vanes

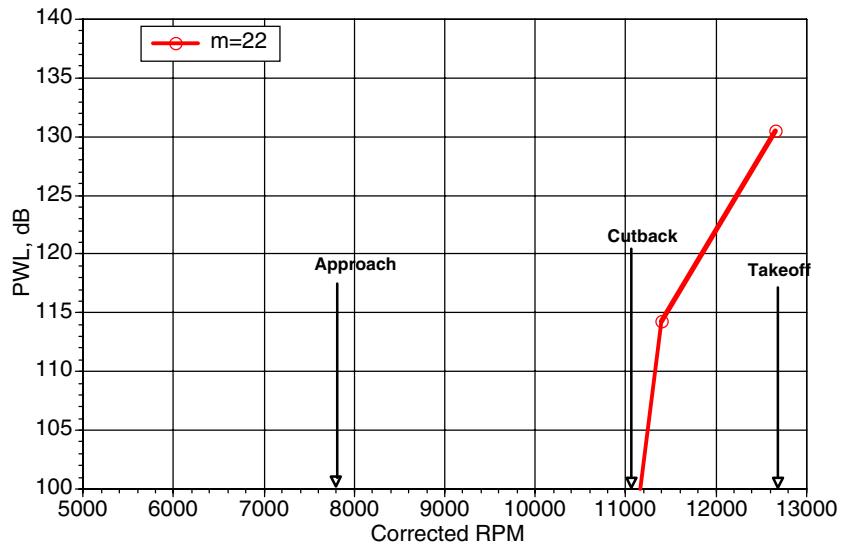
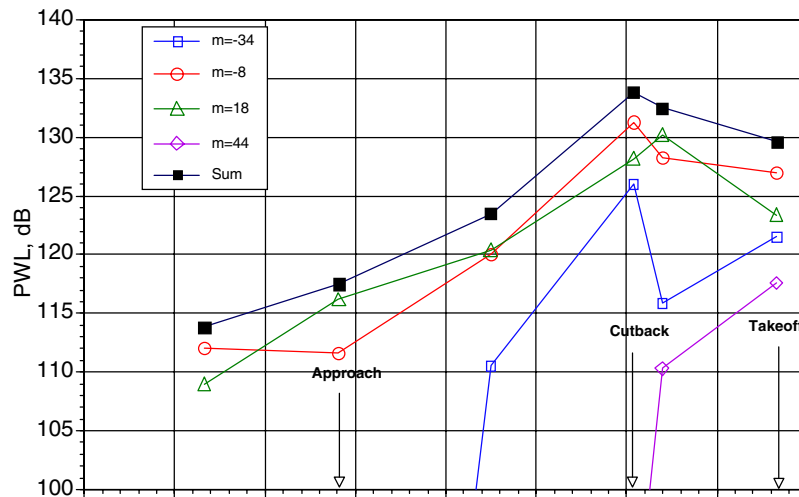
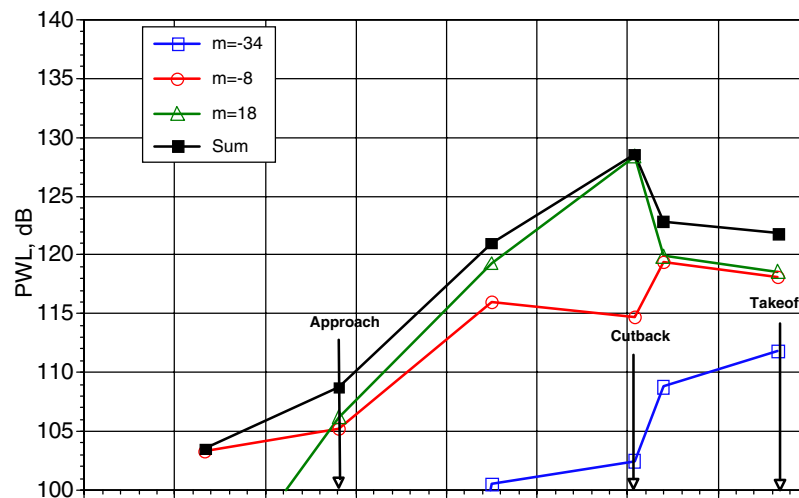


Figure 15. Exhaust BPF mode power variation with speed.

26 Radial Vanes



26 Swept Vanes



54 Radial Vanes

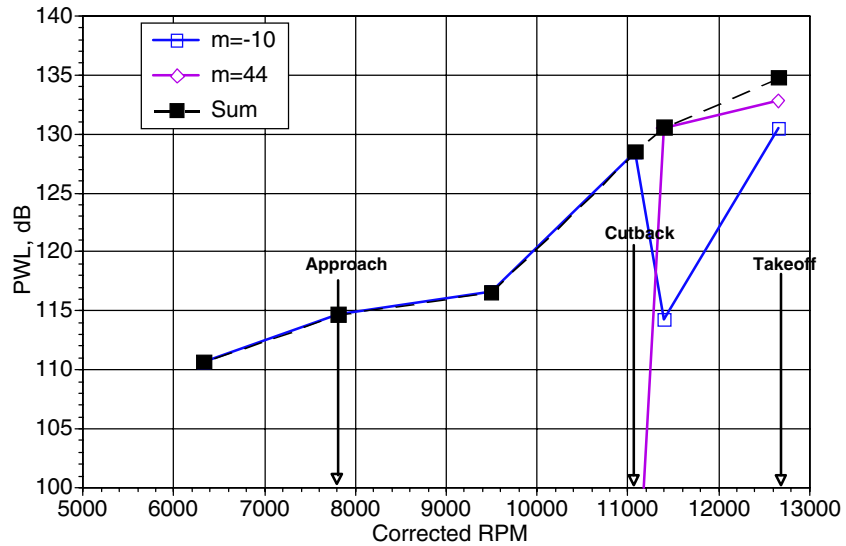
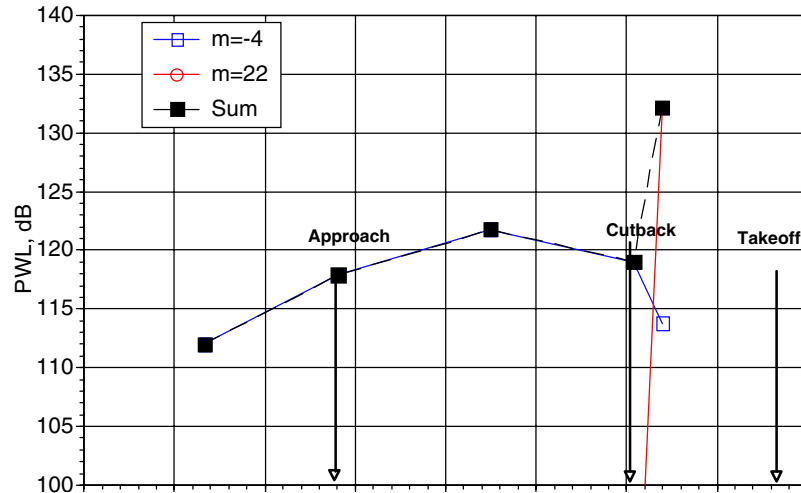
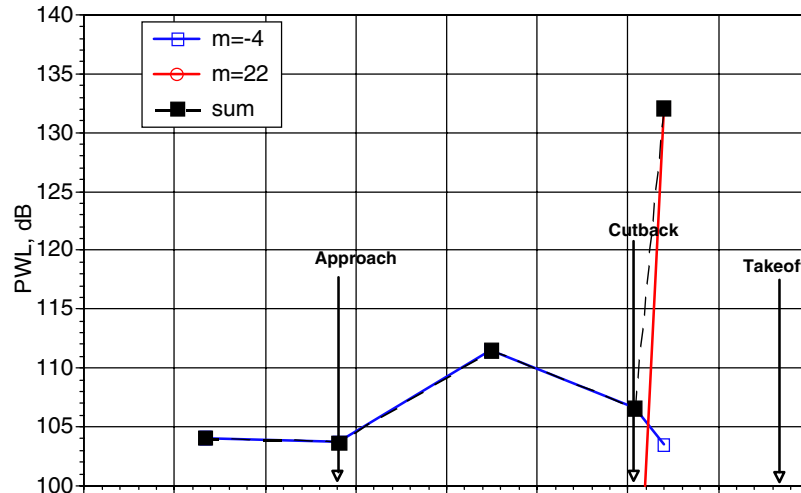


Figure 16. Exhaust 2BPF modal power variation with speed.

26 Radial Vanes



26 Swept Vanes



54 Radial Vanes

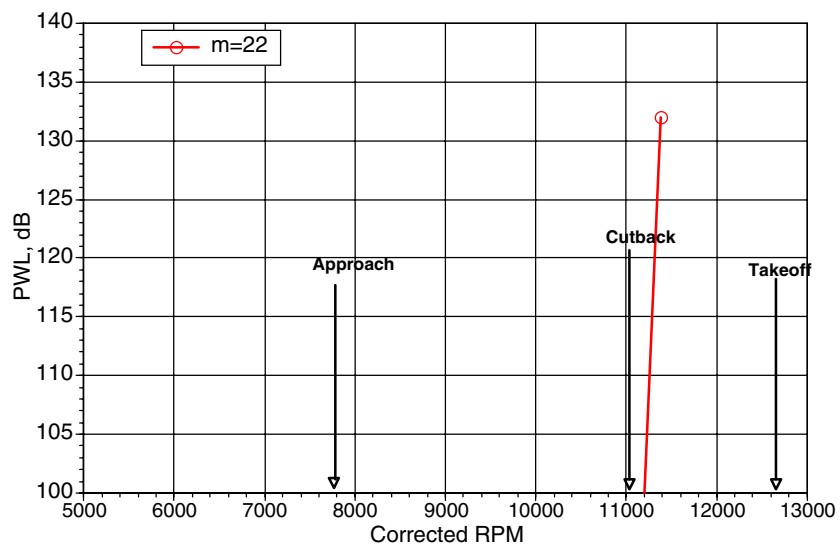


Figure 17. Inlet BPF modal power variation with speed.

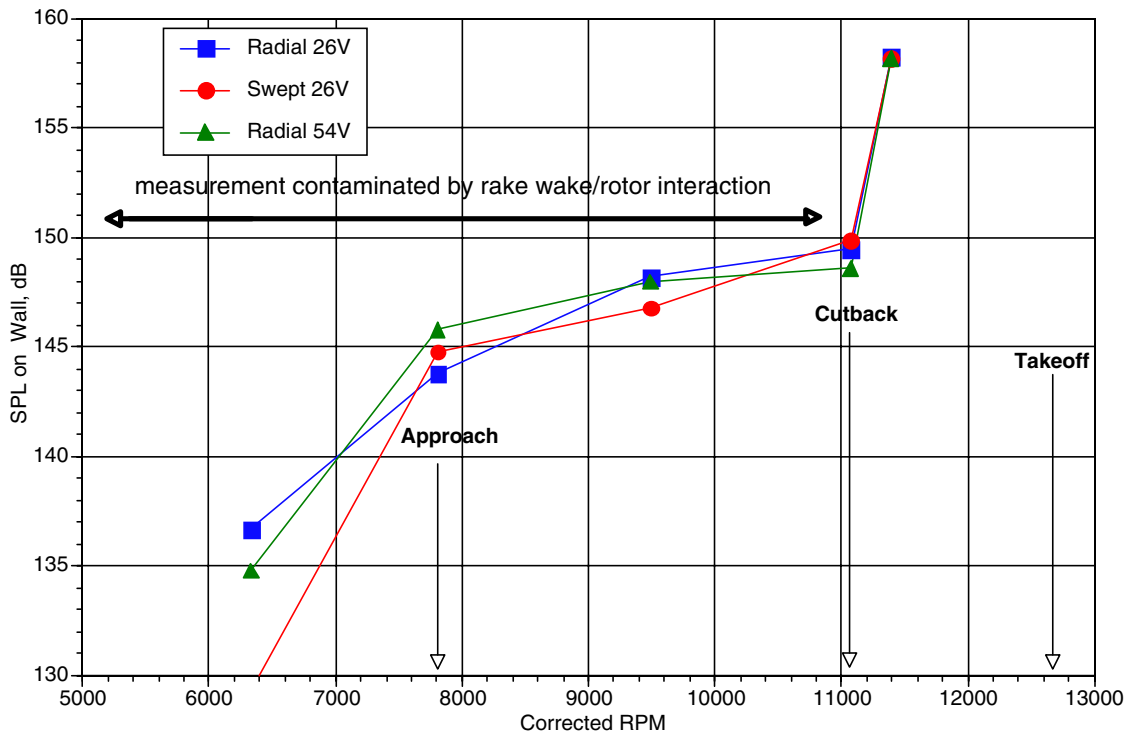
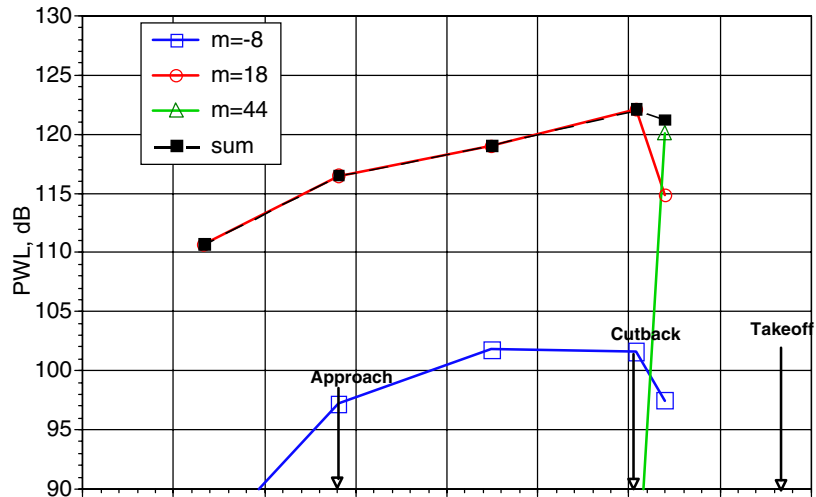
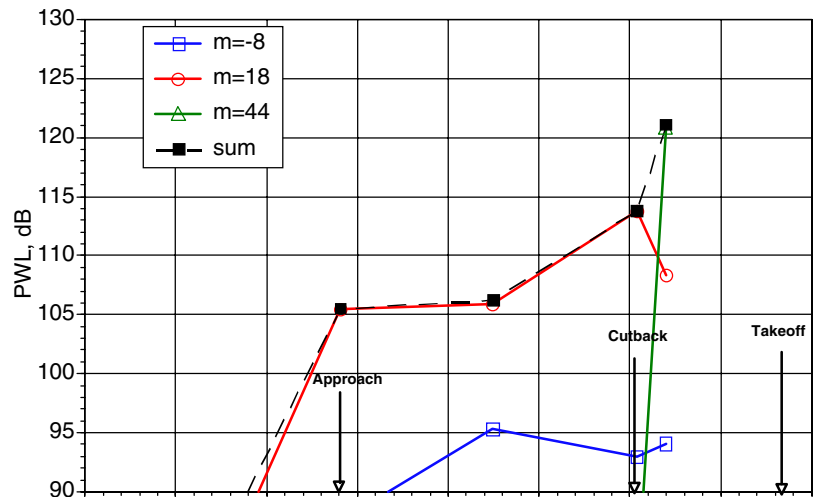


Figure 18. Inlet BPF pressure levels for mode (22,0) as a function of corrected fan speed

26 Radial Vanes



26 Swept Vanes



54 Radial Vanes

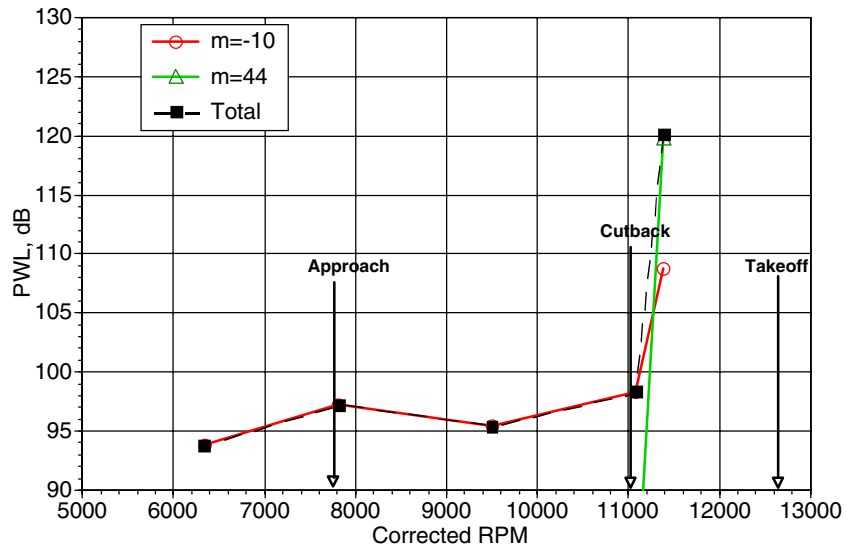


Figure 19. Inlet 2BPF modal power variation with speed.

REPORT DOCUMENTATION PAGE

Form Approved
OMB No. 0704-0188

Public reporting burden for this collection of information is estimated to average 1 hour per response, including the time for reviewing instructions, searching existing data sources, gathering and maintaining the data needed, and completing and reviewing the collection of information. Send comments regarding this burden estimate or any other aspect of this collection of information, including suggestions for reducing this burden, to Washington Headquarters Services, Directorate for Information Operations and Reports, 1215 Jefferson Davis Highway, Suite 1204, Arlington, VA 22202-4302, and to the Office of Management and Budget, Paperwork Reduction Project (0704-0188), Washington, DC 20503.

1. AGENCY USE ONLY (<i>Leave blank</i>)	2. REPORT DATE May 2002	3. REPORT TYPE AND DATES COVERED Technical Memorandum	
4. TITLE AND SUBTITLE Fan Noise Source Diagnostic Test—Tone Modal Structure Results		5. FUNDING NUMBERS WU-781-30-11-00	
6. AUTHOR(S) Laurence J. Heidelberg			
7. PERFORMING ORGANIZATION NAME(S) AND ADDRESS(ES) National Aeronautics and Space Administration John H. Glenn Research Center at Lewis Field Cleveland, Ohio 44135-3191		8. PERFORMING ORGANIZATION REPORT NUMBER E-13378	
9. SPONSORING/MONITORING AGENCY NAME(S) AND ADDRESS(ES) National Aeronautics and Space Administration Washington, DC 20546-0001		10. SPONSORING/MONITORING AGENCY REPORT NUMBER NASA TM-2002-211594 AIAA-2002-2428	
11. SUPPLEMENTARY NOTES Prepared for the Eighth Aeroacoustics Conference cosponsored by the American Institute of Aeronautics and Astronautics and the Confederation of European Aerospace Societies, Breckenridge, Colorado, June 17-19, 2002. Responsible person, Laurence J. Heidelberg, organization code 5940, 216-433-3859.			
12a. DISTRIBUTION/AVAILABILITY STATEMENT Unclassified - Unlimited Subject Category: 01 Available electronically at http://gltrs.grc.nasa.gov/GLTRS This publication is available from the NASA Center for AeroSpace Information, 301-621-0390.		12b. DISTRIBUTION CODE	
13. ABSTRACT (<i>Maximum 200 words</i>) This investigation is part of a test series that was extremely comprehensive and included aerodynamic and acoustic testing of a fan stage using two different fan rotors and three different stator designs. The test series is known as the Source Diagnostic Test (SDT) and was conducted by NASA Glenn as part of the Advanced Subsonic Technology (AST) Noise Reduction Program. Tone mode measurements of one of the rotors with three different stators were made. The stator designs involve changes in vane count and sweep at constant solidity. The results of both inlet and exhaust tone mode measurements are presented in terms of mode power for both circumferential and radial mode orders. The results show benefits of vane sweep to be large, up to 13 dB in total tone power. At many conditions, the increase in power due to cutting on the rotor/stator interaction is more than offset by vane sweep. The rotor locked mode is shown as an important contributor to tone power when the blade tip speed is near and above Mach one. This is most evident in the inlet when the direct rotor field starts to cuton.			
14. SUBJECT TERMS Ducted fans; Propagation modes; Engine noise; Aeroacoustics		15. NUMBER OF PAGES 27	
		16. PRICE CODE	
17. SECURITY CLASSIFICATION OF REPORT Unclassified	18. SECURITY CLASSIFICATION OF THIS PAGE Unclassified	19. SECURITY CLASSIFICATION OF ABSTRACT Unclassified	20. LIMITATION OF ABSTRACT